Colloid Polym Sci 278:872–877 (2000)

SHORT COMMUNICATION

A. Tsuchida
K. Taguchi
E. Takyo
H. Yoshimi
S. Kiriyama
T. Okubo
M. Ishikawa

Microgravity experiments on colloidal crystallization of silica spheres in the presence of sodium chloride

Received: 20 January 2000
Accepted: 9 March 2000

A. Tsuchida · K. Taguchi · E. Takyo
H. Yoshimi · S. Kiriyama · T. Okubo (✉)
Department of Applied Chemistry
Faculty of Engineering
Gifu University, Yanagido 1-1
Gifu 501-1193, Japan
e-mail: okubotsu@apchem.gifu-u.ac.jp
Fax: +81-58-2932628

M. Ishikawa
Mitsubishi Research Institute Inc
2-3-6 Otemachi, Chiyoda-ku
Tokyo 100-0004, Japan

Abstract Rate coefficients (k) in the colloidal crystallization of monodispersed silica spheres in the presence of sodium chloride are studied in microgravity achieved by parabolic flights of an aircraft. Time-resolved reflection spectroscopy is made with a continuous circulating-type stopped-flow cell system. The k values decrease as the salt concentration increases both at 0 and 1 G and those in microgravity are smaller than those in normal gravity by 16% (maximum), especially in water and in the presence of a small amount of the salt lower than 2×10^{-6} mol/l. The rates in flight at 1 G are larger by 15% (maximum) compared with those at 1 G on the ground. The k values obtained at 0 G, 1 G in flight and 1 G on the ground agree excellently with each other for the suspensions with 3×10^{-6} and 4×10^{-6} mol/l sodium chloride. Disappearance of the downward diffusion of spheres and no convection of the suspensions are important for retardation in microgravity.

Key words Colloidal crystallization kinetics · Microgravity experiments · Salt effect · Reflection spectroscopy

Introduction

The effect of microgravity on the physicochemical properties of most colloidal dispersion systems has not been discussed in detail hitherto. However, we should note that the gravitational effect is significant for the translational diffusion of colloidal particles larger than 0.1 μm and with a density difference of the particles against solvent ($\Delta\rho$) greater than 0.1. The Peclet number (Pe) which is the ratio of the time of sedimentation of a sphere in gravity against that of translational Brownian diffusion, is one of the convenient parameters for determining the gravitational effect compared with Brownian diffusion [1–4].

$$Pe = rS/D_t = (4\pi r^4 \Delta\rho g)/(3k_B T) \quad , \qquad (1)$$

where r is the sphere radius, S and D_t the sedimentation and translational diffusion coefficients, g the gravitational acceleration, k_B the Boltzmann constant and T the absolute temperature, respectively. When $\Delta\rho$ values are taken to be 0.1 and 1, for example, Pe values are evaluated to be 10^{-8} (r = 10 nm), 10^{-4} (100 nm), 1 (1 μm), 10^4 (10 μm), and 10^{-7} (10 nm), 10^{-3} (100 nm), 10 (1 μm), 10^5 (10 μm), respectively.

Microgravity has been achieved by several methods, i.e., the free-fall experiments of a capsule through an evacuated tube (time duration 3–10 s, quality of microgravity about 10^{-5}–10^{-4} G), the parabolic flight of an aircraft (20–30 s, about 0.01 G), shooting a rocket (10–20 min, about 10^{-4} G), space shuttle flight (several days, about 10^{-3} G) and space station experiments scheduled in the near future (several years, about 10^{-3} G).

Some researchers have studied thermodynamics and kinetics properties of colloidal dispersions in microgravity [5]. Vanderhoff et al. [6] have succeeded in preparing monodispersed polystyrene spheres 5–18 μm in diameter with narrower particle size distributions in microgravity than those prepared in normal gravity. A series of

polyacrylamide gels has been synthesized in microgravity [7]. Quite recently Zhu et al. [8] reported the microgravity effect on the morphology of colloidal crystals using the space shuttle Columbia. Our group has made several microgravity experiments on colloidal dispersion systems, such as colloidal crystallization kinetics of single- and two-component spheres in exhaustively deionized aqueous suspensions [9–12], polymerization kinetics of the colloidal silica spheres formed [13], syntheses of nylon vesicles and the rotational relaxation times of anisotropic-shaped particles of tungstic acid colloids [14].

As far as we know, the sedimentation effect for colloidal crystals in normal gravity was first discussed quantitatively by Crandall and Williams [15] and later by Furusawa and Tomotsu [16]. We have studied microscopic and spectroscopic features of colloidal gases, liquids and crystals in sedimentation equilibrium [17–22]. Furthermore, sedimentation and diffusion equilibria of colloidal gases and crystals have been studied [23, 24]. The elastic moduli of colloidal crystals are very low, of the order of 10^{-2}–10^{3} Pa, compared with those of metals, 10^{10} (lead)–10^{12} Pa [15, 16, 18, 25, 26]. Thus, the colloidal structure is distorted easily and even broken by external fields such as a shearing force, an electric field, an elevated pressure, a centrifugal field and even gravity.

Recently, we reported several kinetics studies on colloidal crystallization in normal gravity by reflection spectroscopy and also static and dynamic light scattering measurements [25, 27–29]. Nucleation and crystal growth processes have been analyzed using classical diffusion theories. The nucleation rates increased sharply from 10^{-3} to 10^{3} μm^{-3} s^{-1} when the sphere concentration of colloidal silica of 110-nm diameter increased from a volume fraction, ϕ, of 0.0005 to 0.0026, for example. First and second crystal growth processes were analyzed. The former rate was predominant at low sphere concentrations and increased first and then decreased after passing the maximum as the sphere concentration increased. The latter step was significant at high sphere concentrations and was attributed to the reorientation of colloidal crystals formed in the first step toward the more stable ones. The rate decreased sharply as the sphere concentration increased.

We have performed microgravity experiments on the kinetics analyses of nucleation and growth processes in the colloidal crystallization of silica spheres by the parabolic flights of an aircraft [11]. The crystal growth rates of face-centered cubic lattices decreased in microgravity (0 G) by 25–30% compared with those in normal gravity (1 G). One of the main reasons for the retardation was attributed to the fact that the downward diffusion of spheres, which may enhance the intersphere collision, disappears at 0 G. The crystal growth rates in colloidal alloy crystallization of binary mixtures of monodispersed polystyrene and/or silica spheres having different sizes and/or densities were also studied in microgravity [12]. Microgravity enhanced the crystallization rates substantially up to 1.7 times compared with those at 1 G. The disappearance of the segregation effect in microgravity was the main cause for the enhancement.

We must pay great attention to the fact that physicochemical properties of colloidal crystals are surprisingly sensitive to the ionic concentration of the suspension. The critical sphere concentration of melting, ϕ_c, for example, increased sharply as the ionic concentration increased. The ϕ_c values of the colloidal suspensions coexisting without resins, with resins for several hours and with resins more than 3 weeks were 0.005, 0.001–0.002 and 0.0001–0.0003, respectively [30]. Furthermore, the nucleation and crystallization rates were influenced substantially by the presence of sodium chloride [31]. The induction periods ranged from 0.2 to 1.3 s and increased as the salt concentration increased, which showed that the nucleation rates decreased as salt concentration increased. Furthermore, the crystal growth rate decreased as the salt concentration increased. In this work the microgravity effect on the colloidal nucleation and crystallization has been studied mainly in the presence of sodium chloride.

Experimental

Materials

Monodispersed colloidal silica spheres of CS-82 were kindly donated by Catalysts & Chemicals Ind. Co. (Tokyo). The diameter (d), standard deviation (δ) from the mean diameter, polydispersity index (δ/d) and specific gravity were 103 nm, 13.2 nm, 0.13, and 2.2, respectively. d and δ were determined using an electron microscope (JEM-2000FX, JEOL, Tokyo). The charge density of the strongly acidic groups was 0.38 $\mu C/cm^2$, which was determined by the conductometric titration on an (Wayne–Kerr, Bognor Regis, UK) autobalance precision bridge, model B331, mark II (Bognor Regis, UK) [32]. These sphere samples were purified carefully several times using an ultrafiltration cell (model 202, membrane: Diaflo XM, Amicon Co., Lexington, Mass., USA) and further treated with a mixed bed of cation- and anion-exchange resins [AG501-X8 (D), 20–50 mesh, Bio-Rad] for more than 4 years. The sample suspensions were set in the cell about 4 h before the microgravity measurements and were circulated at a flow rate of 3 ml/min in a flow-type cell. The water used for the preparation of the sample suspensions was obtained from a Milli-Q water system (Milli-RO Plus and Milli-Q plus, Millipore, Bedford, Mass., USA). All the experiments were performed in an air-conditioned room at a temperature around 25 °C.

Reflection spectroscopy

The cell system used, which was almost the same as one reported previously [11], consisted of a quartz observation cell ($40 \times 10 \times 2$ mm) and a peristaltic pump (7524-10, Masterflex, I11., USA) connected by a PharMed tube with low gas permeability. A column of cation- and anion-exchange resins was used only as a reservoir without resins in this work. The pump circulates the colloidal suspension first to the reservoir column, then to the observation cell and finally back to the pump. The flow rate was

usually 3 ml/min to avoid sphere sedimentation as previously described, and the rate was increased to 9 ml/min before the measurements were taken. A light beam from a halogen lamp (LA-150SX, Hayashi, Tokyo) hits the cell wall through an Y-type optical fiber cable and the reflection spectra are taken on a photonic multichannel analyzer (PMA-50, Hamamatsu Photonics, Hamamatsu). When the colloidal suspension is passed into the narrow observation cell, the crystals are melted away by the shear flow. After stopping the flow, crystallization starts. The crystal growth process was followed from the growth of the Bragg reflection peaks. Within 20 s in microgravity 200 time-resolved reflection spectra were taken. The measurements started 0.5 s before the circulation of the colloidal suspension was stopped. Close-up observation of the flow cell was also made with a charge-coupled-device camera (EM-102T, Elmo, Nagoya).

A Mitsubishi MU-300-type jet aircraft was used for the microgravity experiments. Three types of measurements were made for each flight:

1. On the ground at 1 G in a plane before flight.
2. During flight at 1 G to the test area.
3. In microgravity (0 G) during parabolic flights.

Measurements 1 and 2 were made to obtain reference data at 1 G and to examine the slight vibrational effects of the airplane to the kinetics parameters, respectively.

Determination of the nucleation and crystal growth rates

Most kinetics measurements on the colloidal crystallization at comparatively high sphere concentrations including this work have not observed an induction period, after which the crystal growth starts [33]. Thus, the nucleation rates in the classical theory were not obtained for this study. The size of the colloidal single crystals from the homogeneous nucleation, L, is estimated from the intensity of the reflection peak, I [34];

$$I \propto N_{\mathrm{cryst}} L^3 \propto L^3 \quad , \tag{2}$$

where N_{cryst} is the number of single crystals in the reflecting volume, which is directly proportional to the number concentration of crystals in the final stage of the crystallization process, being equal to the total number of nuclei formed in the whole course of crystallization. Thus, the rates of crystallization, v, should be evaluated from the slope in the time dependencies of the cube root of the peak intensities [11]. However, preliminary analyses of the data, where the cube roots of the intensities are plotted against time, gave large uncertainties. Thus, the rate coefficient, k, was introduced instead of v in this work. The k values were obtained as the reciprocal period where the initial linear line in the peak intensities intersects two horizontal lines, which are drawn at the peak intensities at $t = 0$ and 17.5 s, giving initial and final times at $t = t_{\mathrm{i}}$ and t_{f}, respectively, i.e., $k = 1/(t_{\mathrm{f}} - t_{\mathrm{i}})$. In this work, the t_{i} values, which correspond to the induction times for the crystallization, were very close to zero as described previously.

Results and discussion

Colloidal crystallization of the soft-sphere system in aqueous suspensions has been explained successfully based on the effective soft-sphere model [18, 35–41]. Ionic groups on the colloidal surfaces leave their counterions in the suspension and these excess charges accumulate near the surface forming an electrical double layer. The double layer consists of two regions: an inner region composed of adsorbed counterions (the Helmholtz layer) and a diffuse region containing the remainder of the excess counterions (Gouy–Chapman layer). The counterions in the diffuse region are distributed according to a balance between their thermal motion and the forces of electrical attraction with the colloidal spheres. The thickness of the electrical double layer is approximated by the Debye screening length, D_1,

$$D_1 = (4\pi e^2 n/\varepsilon k_{\mathrm{B}} T)^{-1/2} \quad , \tag{3}$$

where e is the electronic charge and ε is the dielectric constant of the solvent. n is the total concentration of free-state cations and anions in suspension and is given by $n = n_{\mathrm{c}} + n_{\mathrm{s}} + n_{\mathrm{o}}$, where n_{c} is the concentration (number of ions per cubic centimeter) of diffusible counterions, n_{s} is the concentration of foreign salt and n_{o} is the concentration of both H^+ and OH^- from the dissociation of water. In order to estimate n_{c} the fraction of free counterions (β) must be known, since many counterions are bound tightly with the ions on the colloidal surface. Note that the maximum values of D_1, both observed and calculated, are very long, about 1 μm in water.

According to the effective soft-sphere model crystal-like ordering of the single-component spheres is formed when the effective diameter (d_{eff}) of the spheres including D_1 is close to or larger than the intersphere distance (D), i.e., d_{eff} [= sphere diameter (d) + $2 \times D_1$] ≥ D. At $\phi = 0.04$ of CS-82 spheres in this work, d_{eff} values were calculated to be 383, 369, 357, 347, and 337 nm at 0, 1×10^{-6}, 2×10^{-6}, 3×10^{-6}, 4×10^{-6}, and 5×10^{-6} mol/l sodium chloride in suspension, respectively. Here, β was assumed to be 0.1. The d_{eff} values were larger than the intersphere distance, 272 nm, which was calculated assuming the sphere distribution of a simple cubic lattice. This supports the validity of the effective soft-sphere model. The validity of the effective soft-sphere model has been supported by the systematic comparison of the d_{eff} and D values hitherto [18, 35–41].

Typical reflection spectra in the course of crystallization of CS-82 spheres at $\phi = 0.04$ and at a sodium chloride concentration of 1×10^{-6} mol/l in normal gravity are shown in Fig. 1. The reflection peak assigned to the primary Bragg reflection peak appeared at 603 nm. The peak wavelength calculated from the sphere concentration was 592 nm. As shown in the figure, the background intensity decreased slightly in the course of crystallization, which is ascribed to the fact that the suspension becomes transparent due to the phase transition to the crystal from the liquid.

The corresponding Bragg reflection spectra in microgravity are shown in Fig. 2. The peak appeared at 602 nm. The spectral patterns were quite similar to each other in gravity and in microgravity.

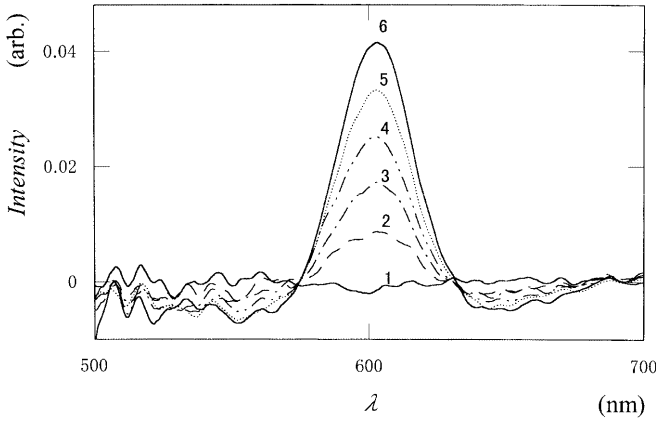

Fig. 1 Reflection spectra during the course of colloidal crystallization of CS-82 spheres at 1 G on the ground at 25 °C. $\phi = 0.04$, [NaCl] = 1×10^{-6} mol/l. *Curve 1*: $t = 0$ s, *2*: 0.5 s, *3*: 1.5 s, *4*: 5.4 s, *5*: 10.8 s, *6*: 17.5 s

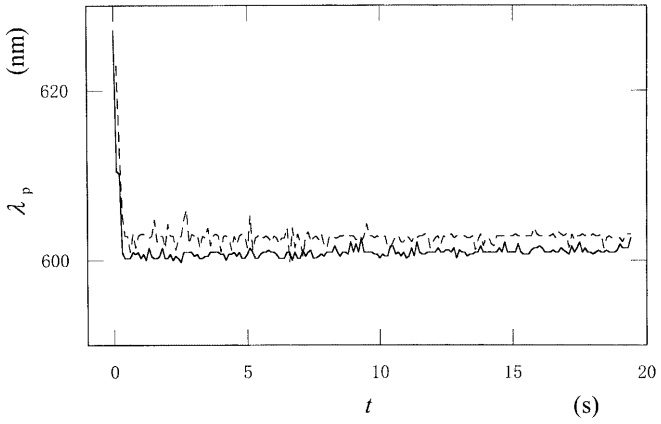

Fig. 3 Time dependence of reflection peak wavelength during the course of colloidal crystallization of CS-82 spheres at 25 °C. $\phi = 0.04$, [NaCl] = 1×10^{-6} mol/l, 0 G (*solid curve*), 1 G on the ground (*broken curve*)

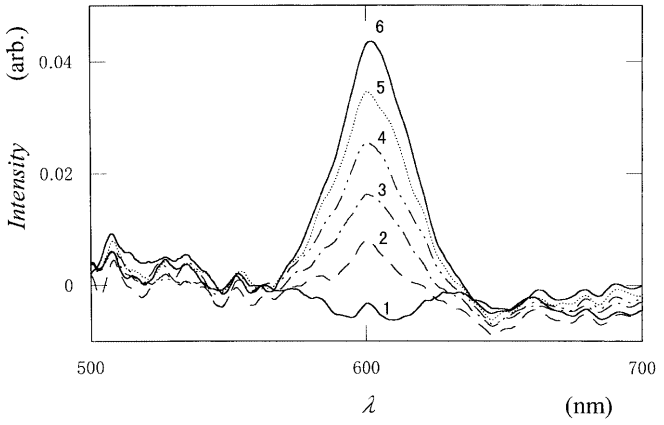

Fig. 2 Reflection spectra during the course of colloidal crystallization of CS-82 spheres at 0 G at 25 °C. $\phi = 0.04$, [NaCl] = 1×10^{-6} mol/l. *Curve 1*: $t = 0$ s, *2*: 0.5 s, *3*: 1.5 s, *4*: 5.4 s, *5*: 10.8 s, *6*: 17.5 s

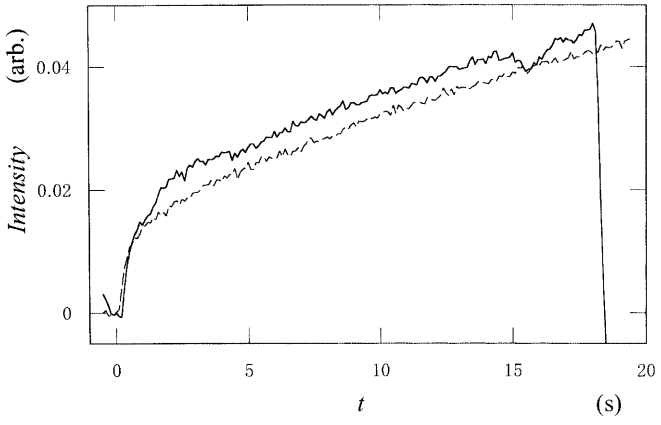

Fig. 4 Reflection intensities during the course of colloidal crystallization of CS-82 spheres at 0 G (*solid curve*), 1 G on the ground (*broken curve*) at 25 °C. $\phi = 0.04$, [NaCl] = 1×10^{-6} mol/l

The time dependencies of the peak wavelengths (λ_p) are shown in Fig. 3. The λ_p values at 0 and 1 G remained constant over the course of crystallization except for the sharp drop at the beginning of crystallization. Within a short period after stopping the suspension flow the broad peak appeared first in a higher wavelength region at about 620 nm. Then the peak wavelengths decreased rapidly to about 600 nm. This shift supports the fact that the metastable and expanded structures are formed first and then the crystals become stabler and denser.

The change in the reflection peak intensities during colloidal crystallization is shown in Fig. 4. As is clear from the figure, there were two steps in the crystal growth processes. The fast step was completed within a few seconds of stopping the flow. The second one showed a slow and linear increase in intensity. As discussed in detail recently [33], the first and the second processes have been assigned to the crystal growth step toward metastable crystals and their reorientation toward stable ones matched with the neighboring crystals and the cell wall, respectively. The second process has often been observed for suspensions of comparatively high sphere concentrations. It should be noted here that in microgravity (solid curve in Fig. 4), the peak intensities decreased abruptly at about $t = 18$ s. This is due to the sharp decrease in the strength of the light source when the microgravity disappeared. Transfer of the heat generated from the lamp surface by convection occurs suddenly at 1 G and the temperature of the lamp drops. As is clear from these curves, no significant difference in the time profile of the peak intensity is observed between normal gravity and microgravity. This suggests that the crystallization mechanism does not change between 0 and 1 G. It should be noted that the nucleation period was not

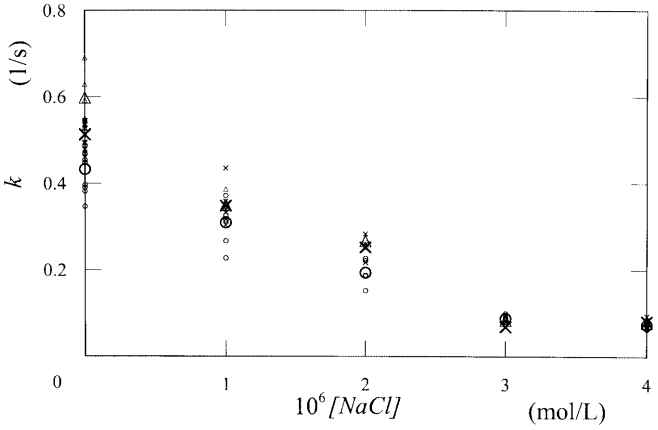

Fig. 5 Apparent growth rates in the colloidal crystallization of CS-82 spheres as a function of NaCl concentration at 25 °C. $\phi = 0.04$, 0 G (○), 1 G on the ground (×), 1 G in flight (Δ)

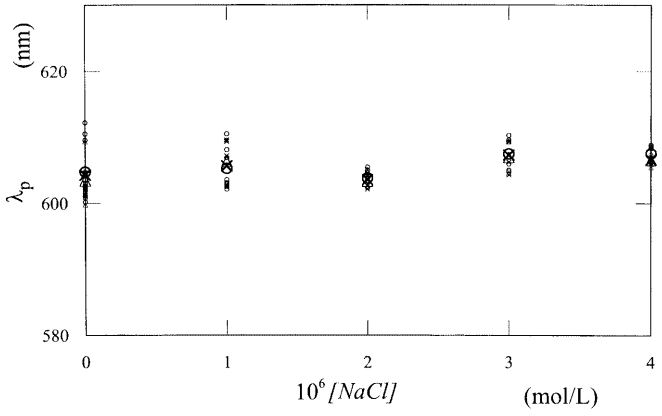

Fig. 6 Final peak wavelength in the colloidal crystallization of CS-82 spheres as a function of NaCl concentration at 25 °C. $\phi = 0.04$, 0 G (○), 1 G on the ground (×), 1 G in flight (Δ)

observable in this work. This is because the sphere concentration was so high, $\phi = 0.04$, and the nucleation period is estimated to be very short, within the experimental errors.

All the data of the crystallization rate coefficient, k, are compiled as a function of salt concentration in Fig. 5. The large symbols show the average values of the repeated experiments. Clearly, the crystallization rates decreased as the salt concentration increased. The main causes for the retardation are ascribed to the thinning of the electrical double layers and the decrease in the electrostatic intersphere repulsive forces as discussed in a previous article [31].

It is interesting to note that the k values at 0 G shown by open circles in the figure were smaller by 16% (maximum) than those at 1 G (crosses) especially at low salt concentrations. The main causes of the retardation are the lack of additional downward translational movement of spheres by gravity and no convection of the suspension at 0 G [11].

The elastic moduli of colloidal crystals are so small that a small shear is enough to melt the crystals. In this work the kinetics effects of small vibrations which are generated by the aircraft engines were examined. The growth rates in flight were larger than those on the ground by about 15%. In a previous article on a deionized suspension [11], the rate coefficients in flight at sphere concentrations higher than 0.003 were also larger than those on the ground. The vibrations may enhance the translational diffusion of the colloidal spheres, and hence the crystallization rate increases. It should be mentioned here that the rate coefficients in the presence of concentrations of sodium chloride higher than 3×10^{-6} mol/l were quite insensitive to the gravitational forces and also to the salt concentration itself. The latter observation has been reported in previous work [31].

The final reflection peak wavelengths are plotted as a function of salt concentration in Fig. 6. No effects of microgravity and vibration were observed. Furthermore, the λ_p values were insensitive to the salt concentration or increased only slightly as the salt concentration increased.

Acknowledgements The authors are grateful to the National Space Development Agency of Japan (NASDA, Tokyo) and the Japan Space Forum (JSF, Tokyo) for their financial support. M. Komatsu and M. Hirai of Catalysts & Chemicals Ind. Co. (Tokyo) are acknowledged for providing the colloidal silica sphere samples. Diamond Air Service Co. (DAS, Toyoyama, Aichi-pref.) is also acknowledged for carrying out the parabolic flights. The quartz glass flow cell was made by Nakamura Glass Co. (Kyoto). The Ministry of Education, Science, Sports and Culture is thanked for Grants-in-Aid for Scientific Research on Priority Areas (A) (11167241) and for Scientific Research (B) (11450367). T.O. is grateful to the late Prof. Emeritus Sei Hachisu for his continuous encouragement for our study on colloidal crystals.

References

1. Hunter RJ (1981) Zeta potential in colloid science. Principles and applications. Academic, London, p 117
2. Russel WB, Saville DA, Schowalter WR (1989) Colloidal dispersion. Cambridge University Press, Cambridge, p 394
3. van de Ven TGM (1989) Colloidal hydrodynamics. Academic, London, p 78
4. Hiemenz PC, Rajagopalan R (1977) Principles of colloid and surface chemistry, 3rd edn. Dekker, New York, p 176
5. Schiffman RA (1988–1996) Experimental methods for microgravity. Materials science research, vols 2–8. TMS CD-ROM library. TMS, Warrendale, Pa
6. Vanderhoff JW, El-Aasser MS, Micael FJ (1986) PMSE Proc Am Chem Soc Div Polym Mater Sci Eng 54:584

7. Briskman V, Kostarev K, Leontyev V, Levkovich M, Mashinsky A, Nechitailo G (1997) Proceedings of the 48th International Astrononical Congress Turin, Italy. International Astronomy Federation, pp 1–11
8. Zhu J, Li M, Rogers R, Meyer W, Ottewill RH, STS-73 space shuttle crew, Russel WB, Chaikin PM (1997) Nature 387:883–885
9. Ishikawa M, Nakamura H, Kamei S, Okubo T, Morita TS, Kawasaki K, Kono Y (1996) J Jpn Soc Microgravity Appl 13:149–157
10. Ishikawa M, Nakamura H, Okubo T, Morita TS, Osada M, Tamaoki H, Kawasaki K, Koshikawa N, Nakamura Y, Nakakura T, Yoda S (1998) J Jpn Soc Microgravity Appl 15 Suppl II:168–172
11. Okubo T, Tsuchida A, Okuda T, Fujitsuna K, Ishikawa M, Morita T, Tada T (1999) Colloids Surf 153:515–524
12. Okubo T, Tsuchida A, Takahashi S, Taguchi K, Ishikawa M (2000) Colloid Polym Sci 278:202–210
13. Okubo T, Tsuchida A, Kobayashi K, Kuno A, Morita T, Fujishima M, Kohno Y (1999) Colloid Polym Sci 277:474–478
14. Okubo T, Tsuchida A, Yoshimi H, Maeda H (1999) Colloid Polym Sci 277:601–606
15. Crandall RS, Williams R (1977) Science 198:293–295
16. Furusawa K, Tomotsu N (1983) J Colloid Interface Sci 93:504–512
17. Okubo T (1990) J Chem Phys 93:8276–8283
18. Okubo T (1988) Acc Chem Res 21:281–286
19. Okubo T (1989) J Chem Soc Faraday Trans 1 85:455–466
20. Okubo T (1990) J Chem Soc Faraday Trans 86:151–156
21. Okubo T (1994) J Phys Chem 98:1472–1474
22. Okubo T (1995) J Chem Phys 102:7721–7727
23. Hachisu S, Yoshimura S (1980) Nature 283:188–189
24. Yoshimura S, Hachisu S (1983) Prog Colloid Polym Sci 68:59–70
25. Okubo T (1994) In: Macroion characterization. From dilute Solutions to complex fluids. ACS Symposium Series 548. American Chemical Society, Washington, DC, pp 346–380
26. Okubo T (1987) J Chem Phys 86:2394–2399
27. Okubo T, Okada S, Tsuchida A (1987) J Colloid Interface Sci 189:337–347
28. Okubo T, Okada S (1998) J Colloid Interface Sci 204:198–204
29. Okubo T (1988) J Chem Soc Faraday Trans 1 84:1163–1169
30. Okubo T (1994) Langmuir 10:1695–1702
31. Okubo T, Tsuchida A, Kato T (1999) Colloid Polym Sci 277:191–196
32. Okubo T (1993) Colloid Polym Sci 271:190–196
33. Okubo T, Ishiki H (1999) J Colloid Interface Sci in press
34. Dhont JKG, Smiths C, Lekkerkerker HNW (1992) J Colloid Interface Sci 152:386–401
35. Baker JA, Henderson D (1967) J Chem Phys 47:2856–2861
36. Wadachi M, Toda M (1972) J Phys Soc Jpn 32:1147–1147
37. Hachisu S, Kobayashi Y, Kose A (1973) J Colloid Interface Sci 42:342–348
38. Brenner SL (1976) J Phys Chem 80:1473–1477
39. Takano K, Hachisu S (1977) J Chem Phys 67:2604–2608
40. Barnes CJ, Chan DY, Everett DH, Yates DE (1978) J Chem Soc Faraday Trans 2 74:136–148
41. Voeglli LP, Zukoski IV CF (1991) J Colloid Interface Sci 141:79–91